# A 0.3GHz to 1.2GHz tunable 4$^{th}$ order switched gm-C Band-Pass Filter with >55dB Ultimate Rejection and out-of-band $IIP_3$ of +29dBm

Milad Darvishi, Ronan van der Zee, Eric Klumperink, Bram Nauta

University of Twente, Enschede, the Netherlands

The trend towards reconfigurable receivers requires on-chip flexible filters that can replace dedicated, bulky and non-tunable filters (e.g. SAW and BAW [1]). Although BAW filters are compatible with silicon processes, their center frequency is sensitive to thickness variation of the piezoelectric material and the achievable tuneability is limited [1]. Other techniques to make RF on-chip Band Pass Filters (BPF) include Q-enhancement, gm-C and N-path. Q-enhancement has several disadvantages such as high area consumption due to inductors which do not obey process scaling, limited tuneability and poor dynamic range [2]. Main drawbacks of gm-C filters are the tradeoff between power consumption, quality factor, center frequency and dynamic range and the need for tuning circuitry [3]. Recently there has been renewed interest in the translational impedance conversion of N-path filters [4-6]. Due to the "transparency" of the passive mixer, baseband impedance is translated to frequencies around the clock frequency $f_{lo}$ [7]. The interesting features of these filters are their direct tuneability with $f_{lo}$, higher quality factor compared to on-chip CMOS LC filters [2], high linearity and graceful scaling with process.

However, N-path filters [6] have two main limitations: 1) The switch resistance $R_{sw}$ limits the ultimate rejection to $R_{sw}/(R_{sw}+R_s)$ (typically 16dB [4]) where $R_s$ is the source impedance; 2) Recent published N-path filters have only second order filtering, and higher orders have only been achieved by cascading[4], still rendering a "round" bandpass filter shape. This paper proposes a new method to increase the order of the BP filter while having a better pass-band

shape compared to [4,6]. It also weakens the effect of switch-resistance on the ultimate rejection to obtain >55dB ultimate rejection in a 65nm chip.

To achieve a higher order filter, we propose the use of subtraction. Suppose we have two second order band-pass filters with equal bandwidth$\left(\frac{\omega_{0,1}}{Q_1} = \frac{\omega_{0,2}}{Q_2}\right)$, but slightly different center frequencies ($\omega_{0,1}$, $\omega_{0,2}$). If we subtract the output of these two filters, 4$^{th}$ order filters with good pass band shape results (see Fig.1).

The 4-path implementation of our filter is shown in Fig.2. The switches in each path are driven by a non-overlapping 25% duty-cycle LO. The combination of baseband capacitors $C_{BB}$ and switches in each path emulate the RLC tanks of figure 1 with center frequency of $f_{lo}$[6]. To shift the center frequency of the two filter sections apart, the use of multiple clocks would give a lot of overhead, so we looked for another way to obtain frequency shifting. In [4], the filter center frequency is shifted by means of a 16-phase switched capacitor technique. One drawback of this technique is that it folds blockers located at $f_{lo}+17\times f_{IF}$ or $f_{lo}-15\times f_{IF}$. Instead, here we use poly-phase gm cells in baseband to shift the baseband admittance from $C_{BB}j\omega$ to $C_{BB}j(\omega \pm \omega_b)$ with $\omega_b = \frac{2g_m}{C_{BB}}$ . N-path passive mixers realize transformation from baseband to $\omega_{0,i} = \omega_{lo} \pm \omega_b$, i=1,2 (see lower part of Fig.2).

To drive two BPF-paths from one source, the input signal needs to be split. Using capacitive splitting via two times $C_s$ as shown in Fig.2 offers several advantages: 1) it isolates the two N-path filters from each other if the impedance of $C_s$ is relatively high compared to 50Ω; 2) it increases the quality factor of each BPF and consequently lowers the value of required $C_{BB}$ for a given BPF-Q; 3) It improves the ultimate rejection of each path. Finally, a second set of switches has been added to further improve the ultimate rejection of each BPF-path (Fig.2).

The filter also features suppression of signals at even harmonics of $f_{lo}$. This is because at even harmonics of the clock frequency, the differential baseband voltages ($V_{I1,2}$ and $V_{Q1,2}$ in Fig.2) are zero. Therefore there will be no frequency shift of the two BPF-sections and the signal is cancelled in the subtraction. The next BPF filter peak will be at the third harmonic of $f_{lo}$. In addition, there is folding back from $3f_{lo}$, $5f_{lo}$, ... to $f_{lo}$[6]. To reduce folding back and filtering at odd ($n\neq1$) harmonics of the $f_{lo}$, a time-invariant wideband and fixed low-pass pre-filter can be used.

For measurement purposes, two buffer stages have been added. The buffer stages and the differential gm stages of the filter are shown in Fig.3. The baseband capacitors $C_{BB}$ are 20pF, made of accumulation-mode N-type MOS capacitors. The on-resistance of the switches is $10\,\Omega$, the series capacitor $C_s$ is 1pF, and the bandwidth of the filter is 21 MHz.

The circuit was realized in 65nm CMOS. The simulated rejection characteristics of a differential 4-path filter [6] ($R_{sw}=5\Omega$ and $C_{BB}=40$pF, the same total capacitor) and the proposed filter have been included for comparison with measurement results (upper part of Fig.4). Clearly, the shape factor and maximum filter rejection are improved significantly. Moreover, to check the out of band filter shape mismatch, 10 samples have been measured (Fig.4, lower part). The measurements in Figure 5 show a well-defined bandpass shape and tuneability from 300MHz to 1.2GHz, with an equivalent quality factor Q changing from 14 to 57. The filter characteristic is quite insensitive to strong out-of-band blockers as shown in Fig.5 for a continuous wave blocker of +2dBm at $\Delta f=+50$MHz from the center frequency. The only visible change in the filter shape is the reduction of rejection at $2f_{lo}$. The static and dynamic current consumption of the filter are 3.2mA from 2.5V and 12.4mA from 1.2V, respectively (at 1GHz). The LO leakage power to the input port is <-60 dBm. The maximum absolute value and the maximum variation of the group

delay of the filter are 70ns and 30ns, respectively. The inband 1-dB compression point of the filter is -4.4 dBm, the inband $IIP_3$ of the filter is +9 dBm and the out-of-band $IIP_3$ is +29 dBm. The input referred rms noise voltage is 2.66nV/√Hz and the noise figure of the filter is 9.5dB (noise of the buffers, estimated from simulation, has been de-embedded from the noise figure). The main contributors to the noise are the 1/f noise of the gm stages and loss in the splitting of the input signal with relatively high impedance capacitors. The filter noise figure is similar to a typical mixer noise figure and hence an LNA will usually be needed in an antenna filter application. Also, this filter might be used as an IF filter for super-heterodyne architecture, where the IF frequency can be adapted to actual interference conditions. The die photo is shown in Fig.7 and the active area of the filter is 0.127 $mm^2$. The filter is compared with [1-6] in Fig.6. We even added filtering-receivers [4,5] in the comparison table. Our filter outperforms Q-enhancement [2] and gm-C [3] filters from a linearity, noise and tuneability point of view. Compared to [5, 6], it has better pass-band shape and much higher rejection at RF frequencies. Moreover, this work has comparable out of band rejection and better pass band shape compared to [4] where most of the filtering is done in IF stages and the RF filtering is limited. To the knowledge of authors, this filter is the most compact one published with steep filter shape, high ultimate rejection and good linearity, without requiring a complete receiver.

*Acknowledgements:*

This research is supported by STW. We thank STMicroelectronics for Silicon donation and CMP for their assistance. Also thanks go to G. Wienk, H. de Vries and M. Soer for their helpful contributions.

*References:*

[1] Stephane Razafimandimby; Cyrille Tilhac; Andreia Cathelin; Andreas Kaiser; Didier Belot, "An Electronically Tunable Bandpass BAW-Filter for a Zero-IF WCDMA Receiver," *Solid-State Circuits Conference, 2006. ESSCIRC 2006. Proceedings of the 32nd European*, vol., no., pp.142-145, Sept. 2006

[2] Soorapanth, T.; Wong, S.S., "A 0-dB IL 2140±30 MHz bandpass filter utilizing Q-enhanced spiral inductors in standard CMOS," *Solid-State Circuits, IEEE Journal of* , vol.37, no.5, pp.579-586, May 2002

[3] Ha Le-Thai; Huy-Hieu Nguyen; Hoai-Nam Nguyen; Hong-Soon Cho; Jeong-Seon Lee; Sang-Gug Lee , "An IF Bandpass Filter Based on a Low Distortion Transconductor," *Solid-State Circuits, IEEE Journal of* , vol.45, no.11, pp.2250-2261, Nov. 2010

[4] Mirzaei, A.; Darabi, H.; Murphy, D., "A low-power process-scalable superheterodyne receiver with integrated high-Q filters," *Solid-State Circuits Conference Digest of Technical Papers (ISSCC), 2011 IEEE International* , vol., no., pp.60-62, 20-24 Feb. 2011

[5] Andrews, C.; Molnar, A.C., "A Passive Mixer-First Receiver with Digitally Controlled and Widely Tunable RF Interface," *Solid-State Circuits, IEEE Journal of*, vol.45, no.12, pp.2696-2708, Dec. 2010

[6] Ghaffari, A.; Klumperink, E.A.M.; Soer, M.C.M.; Nauta, B., "Tunable High-Q N-Path Band-Pass Filters: Modeling and Verification," *Solid-State Circuits, IEEE Journal of*, vol.46, no.5, pp.998-1010, May 2011

[7] L. E. Franks and I. W. Sandberg, "An alternative approach to the realization of network transfer functions: The N-path Filters," *Bell Sys. Tech. J.*, vol. 39, pp. 1321-1350, Sep. 1960.

**Captions:**

**Fig.1: Subtracting the output voltage of two 2nd order BPFs with slightly different center frequency to create a $4^{th}$ order BPF**

**Fig.2: $4^{th}$ order switched gm-C BPF**

**Fig.3: The complete filter schematic with buffer stages for measurements**

**Fig.4 : Comparison of filter measurements with simulation and with a simple 4-path filter transfer (top); measured out-of-band filter shape mismatch for 10 samples (bottom)**

**Fig.5: Measured tuneability of the filter and the filter characteristics w/wo +2dBm CW blocker at Δf=+50MHz from the center frequency**

**Fig.6: Comparison Table**

**Fig.7: Chip Micrograph**

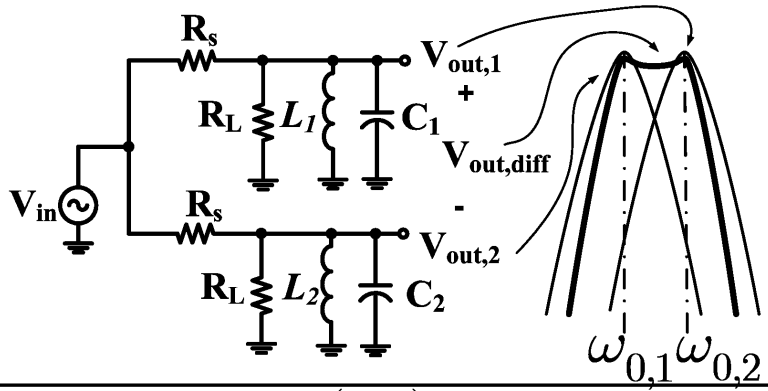


$$\frac{V_{out,i}}{V_{in}} = \frac{R_L}{R_L+R_s} \times \frac{\left(\frac{\omega_{0,i}}{Q_i}\right)\times s}{s^2+\frac{\omega_{0,i}}{Q_i}s+{\omega_{0,i}}^2}, i=1,2$$

$$\frac{V_{out,diff}}{V_{in}} = \frac{R_L}{R_L+R_s} \times \frac{\omega_{0,2}\omega_{0,1}\left(\frac{\omega_{0,2}}{Q_1}-\frac{\omega_{0,1}}{Q_2}\right)\times s}{\left(s^2+\frac{\omega_{0,1}}{Q_1}s+{\omega_{0,1}}^2\right)\left(s^2+\frac{\omega_{0,2}}{Q_2}s+{\omega_{0,2}}^2\right)}$$

**Figure 1: Subtracting the output voltage of two 2nd order BPFs with slightly different center frequency to create a 4th order BPF**

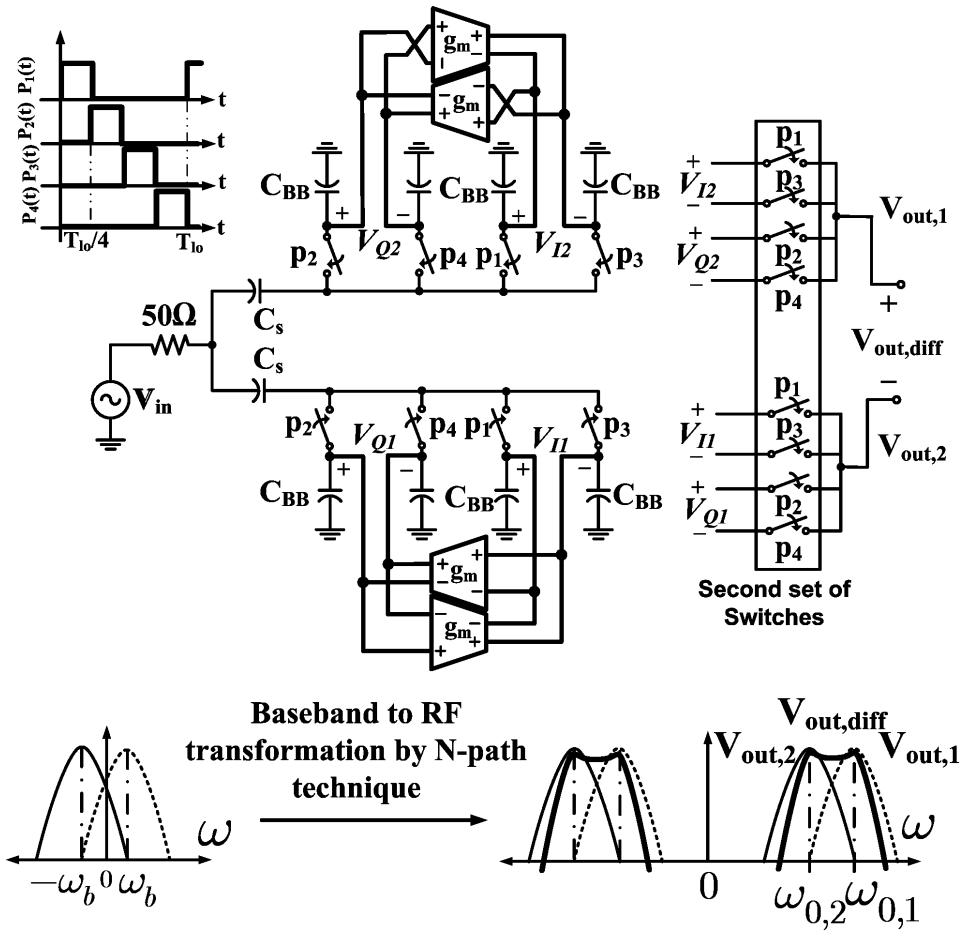


**Figure 2: 4th order Switched $g_m$-C BPF**

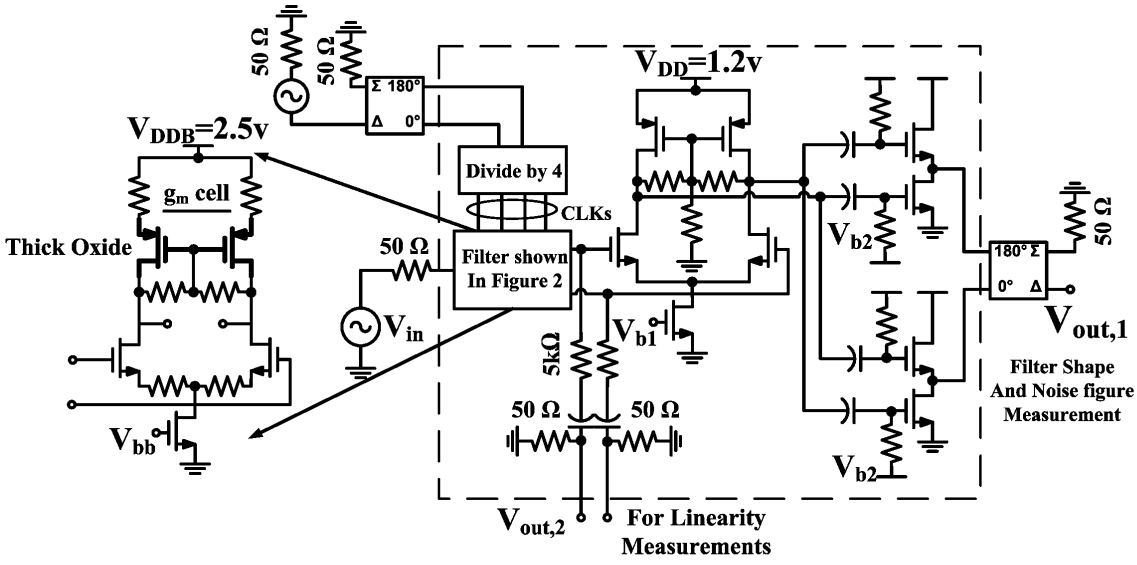


**Figure 3: The complete filter schematic with buffer stages for measurements**

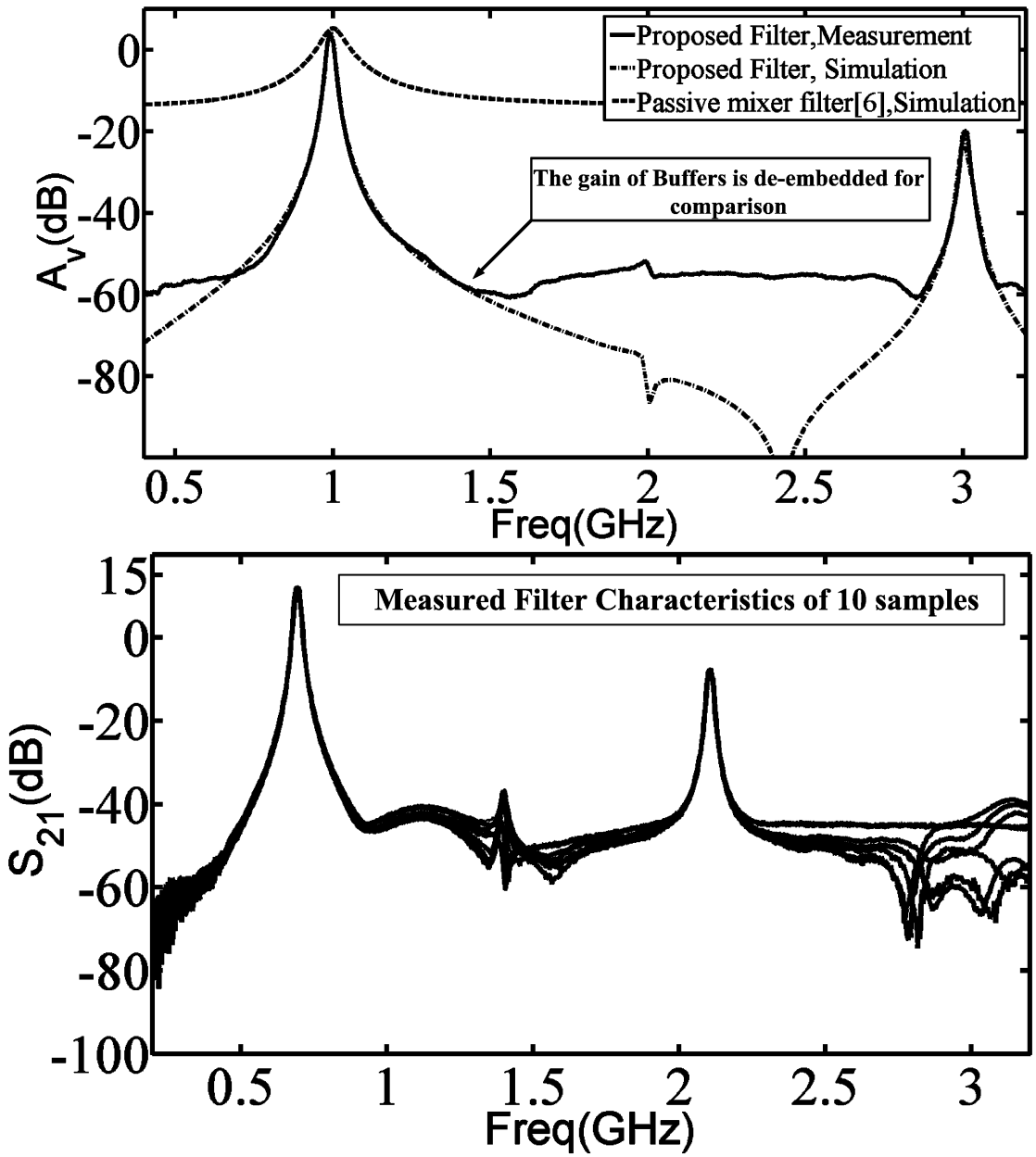


**Figure 4: Comparison of filter measurements with simulation and with a simple 4-path filter transfer (top); measured out-of-band filter shape mismatch for 10 samples (bottom)**

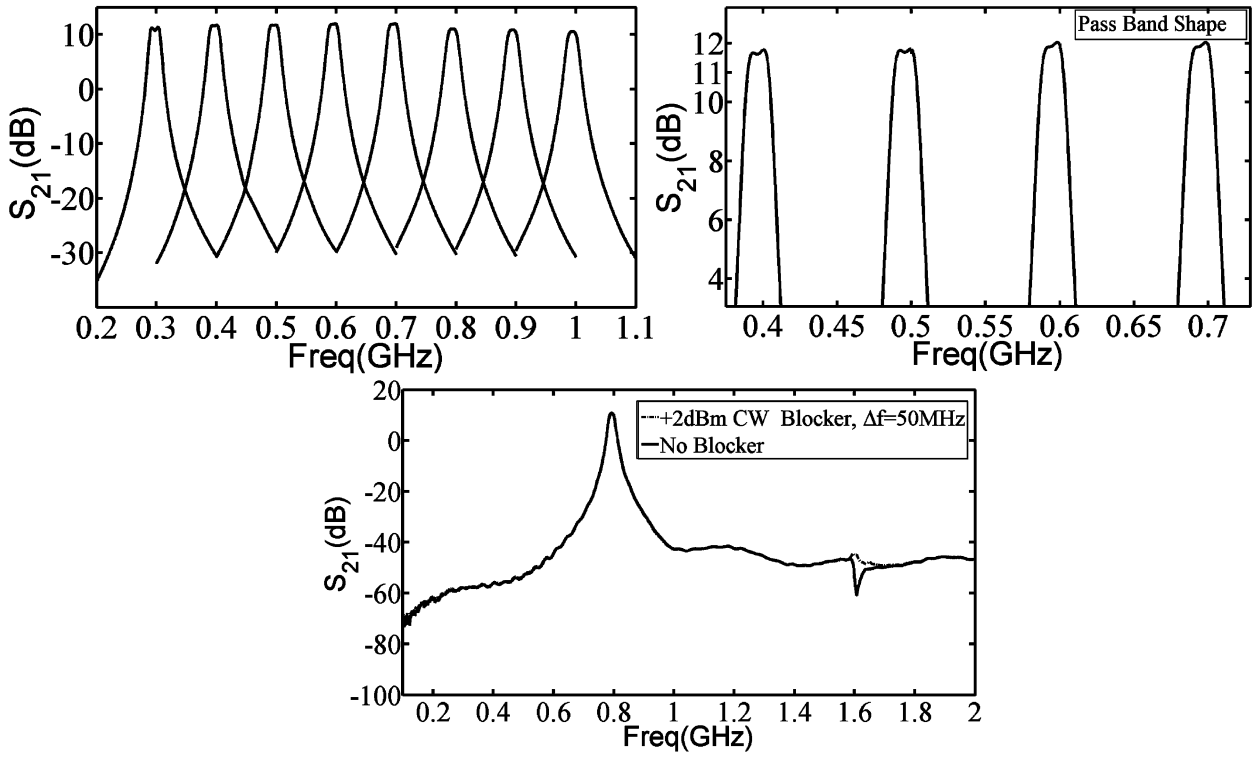


**Figure 5: Measured tuneability of the filter and the filter characteristics w/wo +2dBm CW blocker at Δf=50MHz from the center frequency**

| | [4] | [5] | [6] | [3] | [2] | [1] | [This work] |
|---|---|---|---|---|---|---|---|
| Type | Receiver | Receiver | Filter | Filter | Filter | Filter | Filter |
| Technology[g] | 65nm | 65nm | 65nm | 65nm | 250nm | SiGe: BiCMOS250nm BAW piezoelectric | 65nm |
| Center Frequency(GHz) | 2.14 | 0.05-2.4 | 0.1-1 | 0.08 | 2.14 | 2.14 (±0.15%) | 0.3-1.2 |
| Order of filter | 6 | 2 | 2 | 4 | 6 | 4 | 4 |
| BW(MHz) | 4 | 20 | 35 | 10 | 60 | 60 | 21 |
| Gain (dB) | +55[k] | +70[k] | -1 | +2 | 0 | -9 | +3.5[h] |
| Ultimate Rejection (dB) | 48[d] | 13[j] | 16[c] | 32 | ? | 28 | 55 |
| $P_{1dB}$(in-band)(dBm) | ? | ? | 2 | ? | -13.4 | ? | -4.4 |
| $IIP_3$(in-band)(dBm) | -8.5 | -67 | +19 | -2 | -4.9 | +35 | +9 |
| $IIP_3$(out-of-band)(dBm) | ? | +25 | ? | ? | ? | ? | +29[L] |
| NF(dB) | 2.8[e] | 5.5 | 5.5 | 21.5 | 19 | 9[f] | 9.5[a] |
| Active Area($mm^2$) | 0.76 | 2.5 | 0.07 | 0.25 | 3.51 | 6.65 | 0.127 |
| Max. Ripple(dB) | N.A | N.A | N.A | 0.1 | 0.7 | 1.5 | 0.5 |
| Power Consumption(mW) | 34.2 | 60 | 18 | 13.2 | 17.5 | 7 | 17.6[b] |

[a] Buffers noise contribution is de-embedded($V_{in,n,rms}$=2.66nV/$\sqrt{Hz}$).
[b] 3.2mA static and 12.4 mA dynamic current consumption @ 1GHz
[c] $R_{sw}$=5Ω
[d] It is achieved by cascading 3 BPF, of which most filtering is done in IF.
[e] 10dB on-chip passive gain in Front
[f] Estimated from the loss of filter
[g] CMOS, unless otherwise stated.
[h] De-embedding the buffer's gain.
[i] Calculated from $S_{11}$
[k] Whole receiver gain
[L] Δf=50MHz

**Figure 6: Comparison Table**

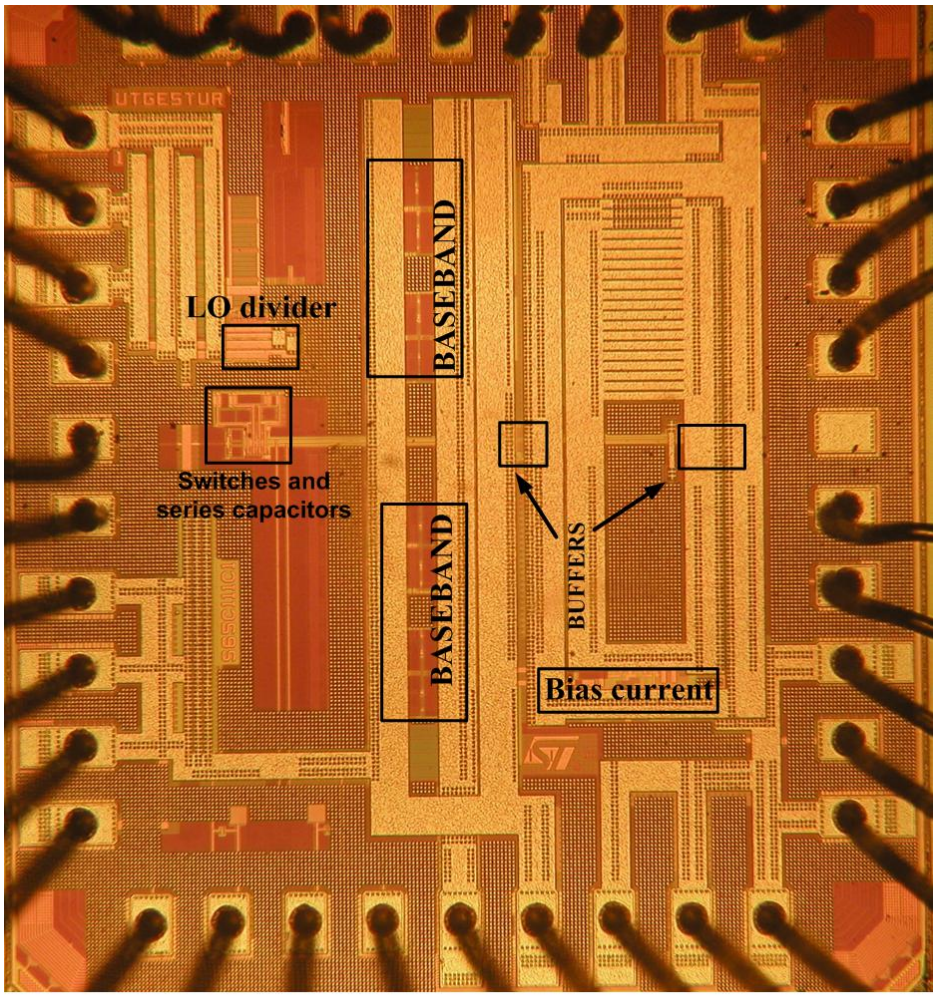


**Figure 7: Chip Micrograph**